EFFECT OF WALL BASE ROTATION ON
BEHAVIOR OF REINFORCED CONCRETE FRAME-WALL BUILDINGS

Daisuke Kato (I)
Hideo Katsumata (II)
Hiroyuki Aoyama (III)
Presenting Author: D. Kato

SUMMARY

This paper reports the tests of multistory frames including a base rotating wall under lateral load reversals. The wall base rotation limited the input forces to the structural system and prevented damage in the wall. The beams, however, were forced to deform much during the wall rotation. A mathematical model was developed to simulate the inelastic behavior of frame members and the uplifting rotation of a structural wall at its base.

INTRODUCTION

Recent earthquake resistant design concept places explicit emphases on the inelastic deformation and energy dissipation capacities in addition to long-time accepted lateral load resisting capacity. Regarding to the behavior of the structural wall in a low-rise reinforced concrete building, three basic modes of failure have been identified: (a) shear failure, (b) flexural failure, and (c) base rotation. Of these three modes, the first two have been studied extensively in the past. In recent years some researchers reported on the base rotating shear walls [Refs. 1,2,3]. However, the effect of base rotation of a structural wall on the behavior of a reinforced concrete frame building is not clearly understood. This paper examines the effect of wall base rotation on the behavior of frames through static load reversal tests, paying special attention to the effect of connecting beams and the wall support conditions.

TEST PROGRAM

In order to understand the effect of the base rotation of a structural wall on the behavior of a reinforced concrete(R/C) frame building. An arbitrary three-story R/C building with an one-bay structural wall on footing foundation was chosen to be a prototype structure. The beams directly connected to a wall may be most significantly affected by the wall uplifting base rotation. Hence the two-story three-bay portion of the frame with the structural wall in the central span was isolated from the prototype structure, the concentrated lateral load being assumed to act at the second floor level to simulate the same base overturning effect under the first mode oscillation. The gravity loads were assumed to be carried by the columns.

(I) Graduate Student, Department of Architecture, University of Tokyo, Japan

(II) Ohbayashi-gumi, Ltd., Tokyo, Japan

(III) Professor, Department of Architecture, University of Tokyo, Japan

Three fifth-scale specimens were constructed. The wall was designed to fail by base rotation in all specimens. Variables in the three specimens were the failure modes (flexure or shear) of connecting beams and the support conditions (rigid or flexible) under the column footings. Specimen FR (flexural beams on rigid foundation) and specimen SR (shear beams on rigid foundation) were supported on rigid steel base. Specimen FD (flexural beams on deformable foundation) was supported on 100 mm-thick hard rubber pads. Dimensions and reinforcement of the specimens are shown in Fig. 1. Details of cross sections of members are shown in Fig. 2. The average compressive strength of the concrete was 27.5 MPa. The average yield stresses of the deformed and plain bars were 367 and 235 MPa, respectively. The elastic modulus of hard rubber under uniaxial compression was approximately 28.1 MPa.

Reversing lateral load was applied statically at the top of the second story wall by a hydraulic jack through high-strength steel rods (Fig. 1). The constant-amplitude axial gravity loads were applied to the columns corresponding to the first-story design axial stress of 2.94 MPa. The movement of the wall footings was restrained by vertical rollers so that the wall footings were free to uplift when the gravity load was overcome by the overturning effect. The movement of the column footings was restrained by friction between the footings and the base due to the vertical loads.

Except for specimen SR, lateral load was reversed at top deflection angles R equal to approximately 1/200, 1/100, 1/50 and 1/30. The deflection angle, the top displacement divided by overall height, was used to describe the deflection of the test structures in this paper. Test SR was terminated after reversal loading at a deflection angle of 1/60 because the connecting beams were severely damaged in shear.

TEST RESULTS

Load-displacement relations at the top of the three specimens are shown separately in Fig. 3 with solid lines. The three specimens exhibited similar behavior; i.e., (a) "yielding" behavior, (b) sharp stiffness at the commencement of unloading, (c) small residual displacement at complete unloading. The hysteresis relation of a frame was influenced by the failure mode of members; i.e., stable large hysteresis energy was dissipated from a frame consisting of dominantly flexural members, whereas the energy dissipation capability degraded with deformation in a frame consisting of members failing in shear.

Fig. 4 shows crack patterns of the three specimens after the scheduled loading. Major damage occurred in the connecting beams of the frame. Only hair-line shear cracks were observed in the walls. In the beams of specimens FR and FD, wide flexural cracks and compressive crushing of concrete were observed at the beam ends. In the beams of specimen SR, shear cracks were observed at deflection angle of 1/800. With an increse in deflection, the shear cracks developed into splitting cracks along the longitudinal reinforcement near the mid-span and at both ends of the beams. In all specimens a large deformation was imposed on beams connected to a wall when the wall rotated at its base. Therefore, it is particularly important to provide the connecting beams, parallel to as well as perpendicular to the wall, with sufficient deformation and energy dissipation capacities when the wall is to be designed to uplift and rotate about its base.

BEHAVIOR OF INDIVIDUAL BEAMS

The behavior of the three shear wall-frame specimens was significantly affected by the hysteresis characteristics of the beams connected to the base rotating wall. Therefore, four cantilever beam components were tested to study the hysteretic characteristics of the beams used in the frame specimens. The beam components represented beams connected to the wall failing in flexure (specimen BF) and in shear (specimen BS), and base girders connected to the wall footings failing in flexure (specimen GF) and in shear (specimen GS). The dimensions and the material properties of the beam specimens were made comparable to those used in the frame-wall specimens. Reversing lateral load was applied statically to a deflection angle of 1/10, assuming the inflection point of beams to remain at the mid span. The deformed bars used in the beam specimens were taken from the same batch as those used in the frame specimen. The average compressive strength of the concrete was 22.6 MPa.

The load-displacement relations of beam specimens BF and BS at the loading end are shown in Fig. 5 with solid lines. Crack patterns of the beam specimens after test are compared with the corresponding beams of the frame specimens in Fig. 4. Four beam specimens developed crack patterns and failure modes almost identical to those of the frame specimens.

ANALYTICAL MODEL FOR NONLINEAR STATIC ANALYSIS

An analytical model was developed, taking into account the inelastic behavior of frame members and the rotation of the structural wall at its base. Analytical models of the frame specimens are shown in Fig. 6.

The beam or column member was idealized as a perfectly elastic massless line element with two nonlinear rotational springs at the two ends (one component model [Ref. 4]). The wall member was idealized as two vertical line elements (pin-connected elements) with infinitely rigid beams at the top and bottom floor levels and one horizontal spring at the base. The two outside pin-connected elements represented the flexural stiffness of the wall and the horizontal spring at the center line of the wall represented the shear stiffness of the wall (Fig. 6). Vertical spring elements were introduced to reflect the effect of transverse beams to restrain the uplifting or flexural deformation of a wall. The footing under the isolated column was idealized as a pin support with an elastic rotational spring. On the other hand, the footing under a wall boundary column was assumed to be supported by vertical springs at the center of the boundary column line, representing the compressive deformation of the ground. When the footing was uplifted from a rigid ground, however, the spring was assumed to act at the exterior edge of the footing considering the resultant point of the ground reaction. When the gravity load was overcome by the overturning effect, the footing was to be separated; hence, no load was to be carried by the vertical spring.

The hysteresis relations (Fig. 5) were idealized to develop a slip hysteresis model (Fig. 7), which could simulate pinching and degrading resistance characteristics. This model could be used for both shear failing beams and flexural yielding beams by choosing proper parameters. The basic hysteretic rules are as follows; (a) the skeleton is represented by a trilinear relation (dashed line in Fig. 7), (b) pinching and resistance degradation occur only after the first yielding in the direction concerned, (c) after pinching, the response point moves toward the previous maximum response point on the skeleton curve, (d) when the response point reaches the skeleton curve, then the loading stiffness becomes zero. Note that the response point dose not move along the skeleton curve once yielding occurs. In addition to the slip model developed for a beam member, three different hysteresis models were used; i.e., (1) degrading trilinear hysteresis model [Ref. 5] for a column member, (2) axial-stiffness hysteresis model [Ref. 6] for a boundary column of a wall (Fig. 8), and (3) a soil hysteresis model for the foundation under the wall footings (Fig. 9). Moment-rotation relation of beam models were obtained from the beam member tests; the difference in compressive strengths of the concrete of the frame tests and the accompanying beam tests was assumed to be negligible.

The response of the slip hysteresis model under the displacement history observed during the beam tests is plotted in a dashed line and is compared with the observed load-displacement relation in Fig. 5. The stiffness parameters of the hysteresis model were arbitrarily taken to match the observed load deflection curve. A good agreement in the overall shape can be noted between the two hysteresis curves. Therefore, the hysteresis model proposed herein could be used in the following nonlinear analysis of a structure as long as the stiffness parameters are properly chosen. For specimen SR (shear failure type), the lower of the two shear strengths observed in positive and negative loading directions was used to represent the shear strength of the beam. Yield moments of other members were calculated by flexural theory. Calculated and observed ultimate member strengths are listed in Table 1 and Table 2.

ANALYTICAL SIMULATION OF THE TESTS

Nonlinear static analyses were performed to simulate the inelastic behavior of the frame specimens. The same displacement history was imposed on the analytical model and the corresponding test specimen at the top floor.

The calculated load-displacement relations were compared with the test results, separately, for the three specimems in Fig. 3. The calculated load-displacement relation of specimen FR agreed well with that of the test. The base shears at the commencement of the uplifting of the wall in each cycle, at the formation of the collapse mechanism, and at the maximum displacement of each cycle were approximately estimated by the analysis. Both in the analysis and experiment, the specimen FD developed the collapse mechanism when the yielding hinge was formed at the end of the top floor beam. However, the calculated load-displacement relation of specimen FD was somewhat larger than the observed base shear in a small displacement range. The results were sensitive to the modelling of vertical springs under the footing; i.e., the stiffness of the rubber and the position of the spring. Regarding specimen SR, the envelope curve of the calculated relation roughly agreed with that of the test although the beams of specimen SR failed in shear. Calculated maximum base shear agreed well with the observed maximum base shear.

CONCLUSIONS

Main findings are as follows:

The base rotating shear walls with ductile connecting beams can maintain the resistance until the ductile beams fail.

The base rotating shear wall on an elastic ground exhibits lower initial stiffness and maximum resistance compared with the wall on a rigid ground.

Large inelastic deformation is imposed on beams connected to a wall when the wall rotates at its base, so that the connecting beams including footing beams must be provided with sufficient deformation capacity if a wall is to be designed to rotate at its base.

The results of the nonlinear analysis showed good agreement with the behavior of the test structures.

AKNOWLEDGMENT

This study was undertaken in the Department of Architecture, the University of Tokyo. Authors express deepest appreciation for the advices by Professor S. Otani of the University of Tokyo.

REFERENCES

[1] Meek, J.W., "Dynamic Response of Tipping Core Buildings", Earthquake Engineering and Structural Dynamics, Vol.6, 1978, pp.437-454.
[2] Huckelbridge, A.A., and R.M.Ferencz, "Overturning Effects in Stiffened Building Frames", Earthquake Engineering and Structural Dynamics, Vol.9, 1981, pp.69-83.
[3] Priestley, M.J.N., R.J.Evison, and A.J.Carr, "Seismic Response of Structures Free to Rock on their Foundation", Bulletin, New Zealand National Society for Earthquake Engineering, Vol.11, No.3, September, 1978, pp.141-150.
[4] Giberson, M.F., "The Response of Nonlinear Multi-Story Structures subjected to Earthquake Excitation", EERC Report, Earthquake Engineering Research Laboratory, California Institute of Technology, Pasadena, California, 1967.
[5] Otani, S., "Hysteresis Models of Reinforced Concrete for Earthquake Response Analysis", Journal, Faculty of Engineering, The University of Tokyo, vol.XXXVI, No.2, 1981, pp.125-159.
[6] Kabeyasawa, T., H.Shiohara, S.Otani, and H.Aoyama, "Analysis of the Full Scale Seven-Story Reinforced Concrete Test Structures Test PSD-3", Report presented during The Third Joint Technical Coordinating Committee Meeting, Tsukuba, Japan, July, 1982.

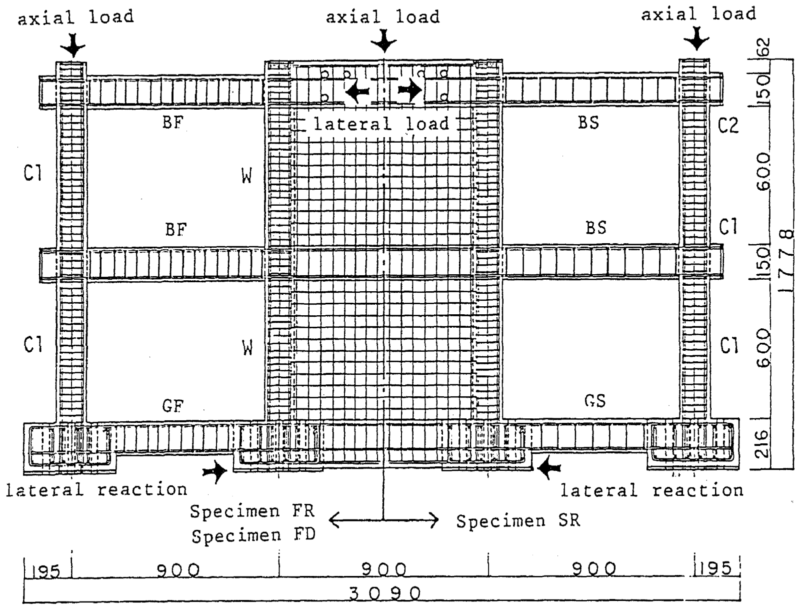

Fig. 1 Dimensions and Reinforcement of Test Structures

Table 1 Calculated Member Strength

Specimen	Maximum Strength (kN-m) Top Tension	Bottom Tension
GF	2.85	2.85
BF	5.98	2.85
GS	4.87	4.87
BS	6.01	5.47
Column	7.68	
Wall	172.	

Table 2 Ovserved Member Strength

Specimen	Maximum Strength (kN-m) Top Tension	Bottom Tension
GF	3.47	3.37
BF	6.16	3.85
GS	6.76	5.23
BS	7.89	6.16

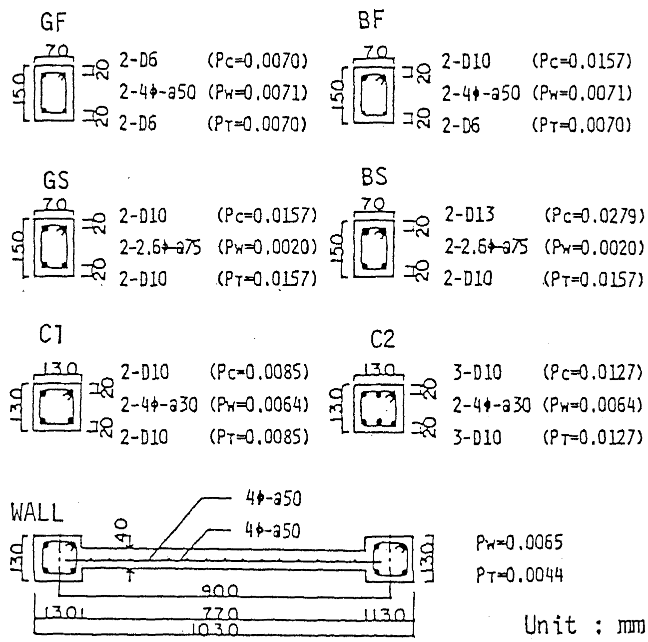

Fig. 2 Details of Cross Sections

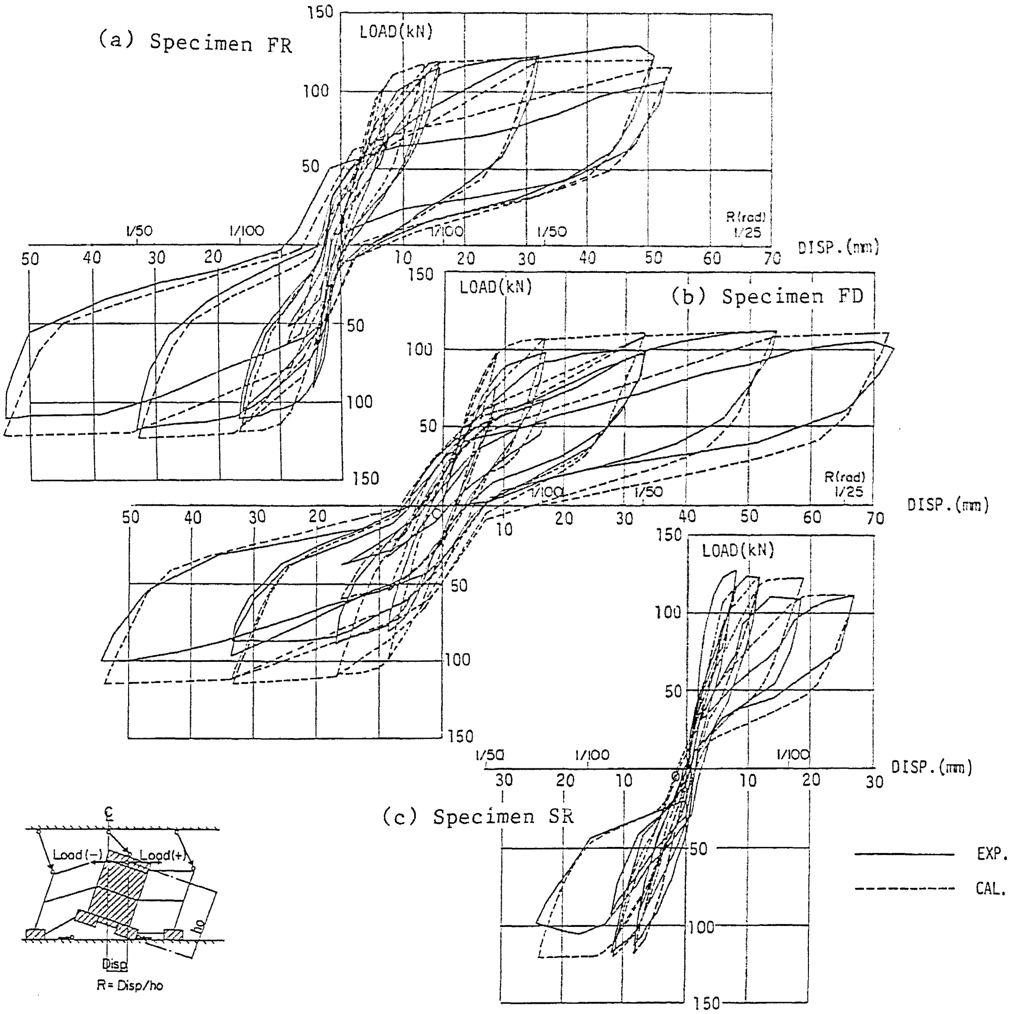

Fig. 3 Load-Displacement Relations of Test Specimens

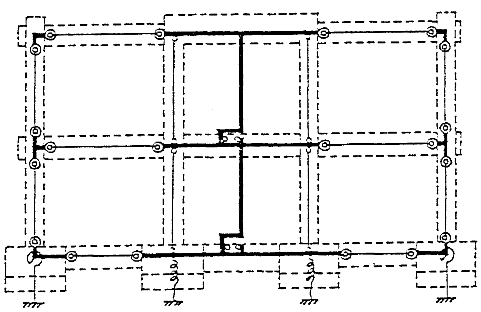

Fig. 6 Analytical Model (Specimen FD)

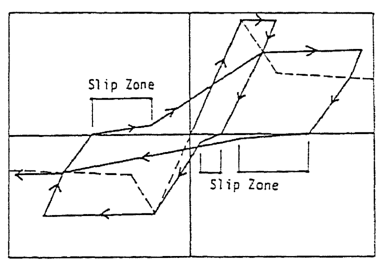

Fig. 7 Hysteresis Models of Beams

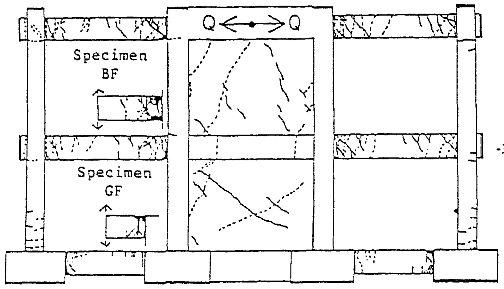

(a) Specimen FR

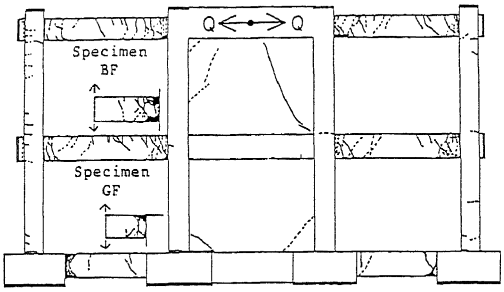

(b) Specimen FD

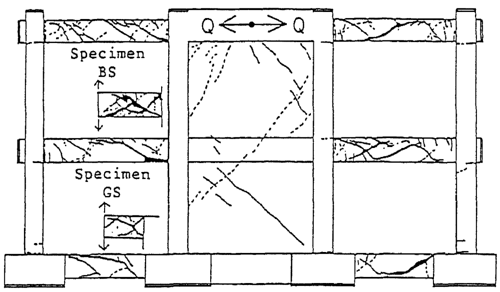

(c) Specimen SR

Fig. 4 Crack Patterns

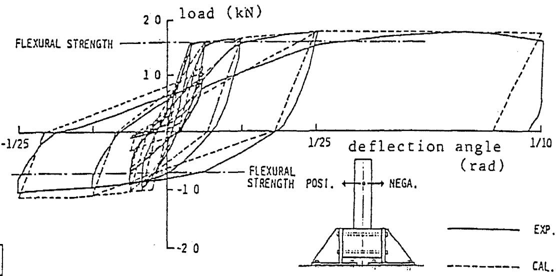

(a) Specimen BF

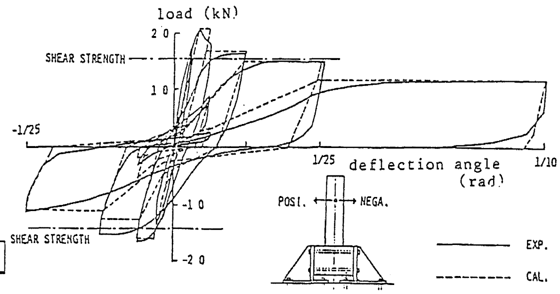

(b) Specimen BS

Fig. 5 Load-Displacement Relations of Beam Specimens

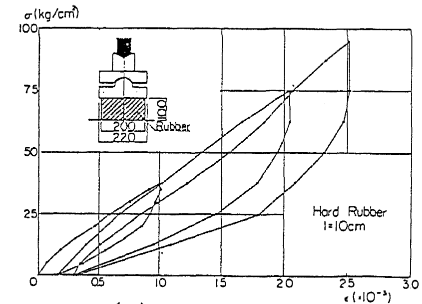

(a) Experiment

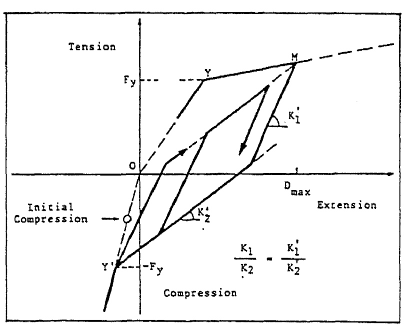

Fig. 8 Axial-Stiffness Hysteresis Model [Ref. 6]

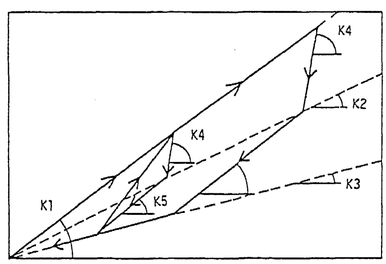

(b) Hysteresis Model

Fig. 9 Characteristics of Hard Rubber and Modelling